

Equivalent Electricity Storage Capacity of Domestic Thermostatically Controlled Loads

Fabrizio Sossan^{a,*}

^a*Distributed Electrical Systems Laboratory, Swiss Federal Institute of Technology of Lausanne (EPFL)*

Abstract

A method to quantify the equivalent storage capacity inherent the operation of thermostatically controlled loads (TCLs) is developed. Equivalent storage capacity is defined as the amount of power and electricity consumption which can be deferred or anticipated in time with respect to the baseline consumption (i.e. when no demand side event occurs) without violating temperature limits. The analysis is carried out for 4 common domestic TCLs: an electric space heating system, freezer, fridge, and electric water heater. They are simulated by applying grey-box thermal models identified from measurements. They describe the heat transfer of the considered TCLs as a function of the electric power consumption and environment conditions. To represent typical TCLs operating conditions, Monte Carlo simulations are developed, where models inputs and parameters are sampled from relevant statistical distributions. The analysis provides a way to compare flexible demand against competitive storage technologies. It is intended as a tool for system planners to assess the TCLs potential to support electrical grid operation. In the paper, a comparison of the storage capacity per unit of capital investment cost is performed considering the selected TCLs and two grid-connected battery storage systems (a 720 kVA/500 kWh lithium-ion unit and 15 kVA/120 kWh Vanadium flow redox) is performed.

Keywords: Power demand, Modelling, Flexibility, Storage.

Nomenclature and Abbreviations

Δt Model simulation sample time (s)

BESS Battery Energy Storage System

SOC State of charge

TCL Thermostatically controlled loads

θ Set of state-space model parameters

A Continuous time state-space system matrix

B Continuous time state-space input matrix

C Continuous time state-space output matrix

E^\downarrow Decrease in electricity consumption with respect to the baseline that a TCL can sustain without violation thermostat bounds (kWh)

*Corresponding author

Email address: fabrizio.sossan@epfl.ch (Fabrizio Sossan)

E^\uparrow	Increase in electricity consumption with respect to the baseline that a TCL can sustain without violation thermostat bounds (kW h)
h	Thermostatic control deadband ($^\circ\text{C}$)
i	Discretized time index
P	Nominal TCL power consumption (kW)
P^\downarrow	Decrease in power consumption that a TCL can achieve (kW)
P^\uparrow	Increase in power consumption that a TCL can achieve (kW)
Q	Hot water demand (L s^{-1})
s	Thermostat state
T	(Air or water) TCL Temperature ($^\circ\text{C}$)
T^*	Thermostatic set-point ($^\circ\text{C}$)
T^o	Outside air temperature ($^\circ\text{C}$)
T^r	Room air temperature ($^\circ\text{C}$)
T^w	Inlet water temperature ($^\circ\text{C}$)
t_i^\downarrow	Time taken by the TCL to pass from T_i to $T^* - h$
t_i^\uparrow	Time taken by the TCL to pass from T_i to $T^* + h$
u	Continuous time state-space input vector
x	Continuous time state-space vector state

1. Introduction

Thermostatically controlled loads (TCLs), like electric space heating, air conditioning, water heating, and refrigeration systems, are characterized by a certain level of flexibility in the consumption thanks to their thermal mass, which allows anticipating or deferring their electricity demand without quick alterations of the temperature to regulate. Although the contribution of a single TCL is negligible, the aggregated and coordinated contribution from a large number of units might have relevant size and be able to impact power system operation.

Achieving nondisruptive controllability (i.e., while respecting consumer comfort) of TCLs has often been advocated in the existing technical literature as a way to provide ancillary services to the electrical grid and tackle the challenge of restoring an adequate level of controllability after the displacement of conventional generation in favor of production from renewables. E.g., in [1–3], TCLs are used to support primary frequency regulation, for voltage regulations in local distribution systems [4], balancing power provision [5, 6], peak shaving and self-consumption [7–11].

Despite the blooming of applications for flexible demand, the current literature does not address the problem of defining specific metrics to quantify the intrinsic flexibility of TCLs. This aspect is of fundamental importance for electric power systems planning because it allows designing response programs for TCLs and quantifying the support they can provide to power system ancillary services. On the contrary for grid-connected electrochemical storage devices (like batteries or fuel-cell/electrolyzer systems), the power and energy capacity ratings allows for a straightforward interpretation of the inherent flexibility and enabled the development of advanced planning strategies (see e.g. [12, 13]) as well as quantification of economic

pay-back times ([14]). The development of similar metrics for the case of TCLs would allow extending existing technical and economic evaluations to the case of flexible demand as well.

The purpose of this paper is presenting a methodology to quantify the equivalent storage capacity of TLCs as if they were conventional grid-connected storage devices. In general, TCLs and conventional storage devices, besides being based on different technologies, do not have equivalent capabilities: whereas the former requires a baseline consumption to guarantee a minimal consumer comfort, the latter does not, and it can even back-feed power if enough charge is available (an important characteristics if considering e.g. power systems restoration procedures). Nevertheless, in certain operational contexts, such as implementation of peak shaving strategies or provision of regulating power, their behavior is comparable: in the same way as storage devices achieve to store electricity for later use, flexible demand can postpone the consumption, thus indirectly achieving the same target, even if for a limited amount of time¹. Therefore, the idea of quantifying the capacity of flexible demand in terms of electricity they can store (equivalent storage capacity) arises naturally in this context, as also considered in [16].

We contribute to the literature by proposing a methodology to evaluate the equivalent storage capacity of common domestic TCLs. The proposed method is applied to evaluate the flexibility intrinsic the operation of four common domestic TCLs (an electric space heating system, electric water heater, freezer and fridge) thanks to thermal models identified from experimental measurements and Montecarlo simulations to reproduce realistic typical operating conditions. The proposed analysis is a valuable tool for system planners to assess the potential of TCLs to support power system operation, allowing for a straightforward comparison with competitive storage technologies, and understanding the amount of flexibility it is possible to harvest from populations of TCLs in given portion of the networks.

The paper is organized as follows: Section 2 introduce the notation, Section 3 states the operational definition of equivalent storage capacity of TCLs, distinguishing among the cases where TCLs are requested to decrease or increase the consumption, Section 4 describes the modelling approach and Montecarlo simulations, Section 5 is for results and discussion, and finally Section 6 states the conclusions.

2. Preliminaries and Notation

As known, a TCL is a device where the state of the active element (like resistors for radiators, or compressors for heat-pump-based loads) can assume two values, *on* or *off*. The thermostat state $s(t)$ at a given time t is determined by a feedback control loop with hysteresis that enables or disables the power consumption when the temperature to regulate falls outside an established dead-band. E.g., for a building space heating TCL, the control law is:

$$s(t) = \begin{cases} \text{on}, & T(t) \leq T^* + h \\ \text{off}, & T(t) > T^* - h \\ s(t - \delta t), & \text{otherwise} \end{cases} \quad (1)$$

where $T(t)$ is the building air temperature, T^* temperature set-point, h temperature hysteresis, and $s(t - \delta t)$ denotes the thermostat previous activation state. Figure 1 exemplifies the temperature dynamics of a TCL and is to introduce the notation used in the following formulation. For convenience in the explanation, we assume that Fig. 1 refers to a TCL for heating application (e.g., space heating), so that the temperature raises when the heating element is active, and vice-versa. Two data points in Fig. 1 are of special interest and are identified by the Cartesian coordinates (t_x, T_x) and (t_z, T_z) :

- Fig. 1, coordinate (t_x, T_x) : the time that the temperature takes to reach the upper thermostatic bound in the case the heater element is kept in the *on* state is denoted by t_x^\uparrow . Conversely, t_x^\downarrow is the time that the temperature takes to reach the lower thermostatic bound if the heating element is switched off. The latter temperature evolution is denoted by the blue dashed line.

¹An additional concern related to the use of flexible demand is the loss of load diversity after a prolonged demand response event, which causes oscillations of the aggregated power consumption, as e.g. shown in [15].

- Fig. 1, coordinate (t_z, T_z) : the time that the temperature takes to reach the lower thermostatic bound in the case the heater element is kept in *off* state is denoted by t_z^\downarrow , whereas t_z^\uparrow is the time that the temperature takes to reach the upper thermostatic bound if the heating element is switched on. The latter temperature trend is denoted by the red dotted line.

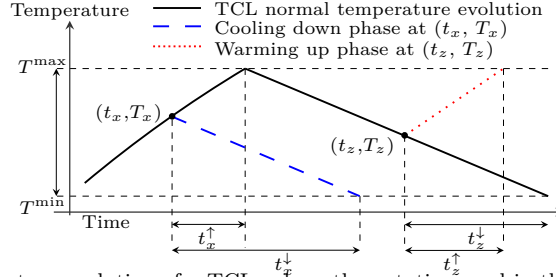


Figure 1: Temperature evolution of a TCL, where the notation used in the text is introduced.

3. Operative definition of equivalent storage capacity of a TCL

Two mainstream control approaches for TCLs and other flexible resources exist: direct and indirect control (see [17] for a more comprehensive review). The former is when an aggregator directly controls the state of the single TCLs (see e.g. [18, 19]), while the most prominent example of the latter case is when TCLs autonomously responds to an open-loop price signal generated in an electricity markets ([20, 21]).

Nevertheless, when considering the operation of a single TCL from a high enough viewpoint, it is possible to recognize two mutually exclusive fundamental cases: after a specific request from the flexible demand operator, a TCL is required to increase, or, alternatively, decrease consumption. Consumption reduction is typically implemented for peak-shaving to meet reduced levels of generation capacity and for lines congestion management (as an alternative to grid reinforcement), whereas both consumption reductions and increases are required to provide up and down-regulation to primary frequency control in cases when the system frequency is below or above the nominal value.

The proposed procedure to evaluate the equivalent storage capacity of a TCL consists in evaluating the consumption which is possible to shift with respect to the baseline² without violating the thermostatic temperature limits. The equivalent storage capacity can be computed analytically for the cases of up and down-regulation, as shown in the next two sections.

It is worth noting that enforcing temperature limits is vital to maintaining consumer comfort. The case of reducing the consumption persistently, or load curtailment, is not considered in this study because it falls outside the concept of nondisruptive controllability of flexible demand.

3.1. Storage capacity for consumption decreasing (for up-regulating power provision)

Decreasing TCL consumption can be achieved by forcing the thermostat state to off. Clearly, this action can be accomplished only if the TCL is in the “on” state. Formally, the power consumption reduction P^\downarrow that can be accomplished at a generic instant of time t_i is:

$$P_i^\downarrow = \begin{cases} P & \text{if TCL is active} \\ 0 & \text{otherwise} \end{cases} \quad (2)$$

where P is the TCL nominal power consumption. With reference to Fig. 1, the first case in (2) is when $t_i = t_x$, and the second when $t_i = t_z$. Assuming the case of $t_i = t_x$ in Fig. 1, the amount of electricity consumption E^\downarrow that can be deferred by turning the consumption off without violating the temperature

²The *baseline consumption* is the TCL consumption in the case no demand response event occurs.

lower value, is the algebraic product between the nominal power consumption of the TCL and the amount of time t_x^\downarrow that the temperature takes to pass from T_x to T_{low} . However, it is to consider that, in the absence of the demand response event, the TCL was going to switch off naturally at the end of the heating phase time $d \cdot T$, which has distance from t_x denoted by t_x^\uparrow . Therefore, the consumption deviation from the baseline demand profile (namely, when no change in consumption is required) is:

$$E_i^\downarrow = \begin{cases} P \cdot \min(t_i^\downarrow, t_i^\uparrow) & \text{if TCL is active} \\ 0 & \text{otherwise,} \end{cases} \quad (3)$$

where the operator $\min(\cdot)$ denotes the minimum value among the two arguments.

3.2. Storage capacity for consumption increasing (provision of down-regulating power)

In contrast to the previous case and provided that the TCL is in the “off” state, an increase of TCL consumption can be achieved by turning it on. Formally, the consumption increase P^\uparrow is:

$$P_i^\uparrow = \begin{cases} 0 & \text{if TCL is active} \\ P & \text{otherwise.} \end{cases} \quad (4)$$

By applying symmetric considerations to those developed for the previous case, the energy capacity available for down-regulation is:

$$E_i^\downarrow = \begin{cases} 0 & \text{if TCL is active} \\ P \cdot \min(t_i^\uparrow, t_i^\downarrow) & \text{otherwise} \end{cases} \quad (5)$$

4. Methods

The focus in this work is quantifying the equivalent storage capacity inherent the operation of selected TCLs. This is performed by, first, simulating the temperature evolutions of the TCLs by using dynamic thermal models, which are introduced in subsection 4.1. Simulations are performed by adopting a Monte Carlo approach with the objective of reproducing scenarios representative of the typical operating conditions of TCLs, as explained in subsection 4.2. Finally, as described in 4.3, once the temperature profiles are known, the equivalent storage capacity of each TCLs is evaluated by applying the definition previously provided in Section 3.

The TCLs considered in this analysis are an electric space heating unit, electric water heater, freezer and fridge. They were selected because, besides being the most common flexible appliances in a household context, are those available in Power Flexhouse³ and for which it was possible to identify and validate dynamic thermal models from experimental measurements. The main characteristics of the experimental units used for the model identification are summarized in Table 1.

4.1. Thermal Models of TCLs

4.1.1. Introduction to grey-box models

According to the taxonomy described in [23], models for thermal electric loads can be grouped into three categories: white, grey, and black-box. Respectively, these are according to if the model is built by applying physical first principles, it relies on simplified physical description of the process with parameters estimated from measurements, or it is entirely identified from measurements, with no hypothesis on the structure of the process generating them. While the former solution is effective and delivers accurate temperature estimations, it comes at the cost of a high complexity and it requires the values of a large number of parameters. On the other hand, black-box models deliver quality predictions only around the training point

³Power Flexhouse is the experimental facility of DTU Elektro for testing demand side control strategies, see [22].

Table 1: Characteristics of the considered TCLs

TCL	Volume	Nominal power consumption P [kW]
Space heating	125 m ² × 2.8 m	10
Water heating	30 L	1.2
Freezer	333 L	0.06
Fridge	60 L	0.08

and need frequent re-training. Grey-box models trade a detailed representation of the physical process to model for an increased tractability level and are often adopted in application to predictions and control, see e.g. [24–26]. Especially, they have the advantage of having parameters identifiable from experimental measurements. Therefore they can be applied even in the absence of the complete knowledge of the system.

The dynamic thermal models used in this study are grey-box identified from experimental measurements, and they are from the existing technical literature [10, 24, 27, 28]. For the sake of clarity, their formulation, identification process, and structure are summarized in paragraphs 4.1.2, 4.1.3 and 4.1.4-4.1.7, respectively. For a thoughtful description of the identification and validation processes, the interested reader is referred to the referenced literature.

It is worth noting that the models considered in this study were originally developed for the purpose of providing early time temperature predictions (typically from minutes to a few hours, depending on the TCLs) rather than for simulations. However, their use for simulation is justified in this context because the time range of their flexibility (namely, the duration for which they can defer or anticipate consumption without violating consumer comfort) is of the same order of magnitude.

4.1.2. General formulation of the models

Models are developed by applying the the thermal equivalent circuit approach, which considers the temperature and heat of a thermal system as the voltage and current of an electric circuit. They are of the third order (unless the water heater, for which a first order model is used, as justified in the following). Compared to lower order, higher order models are able to capture more accurately the thermal dynamics induced by the different thermal masses of the TCLs. Models are formulated and using the continuous time state-space representation, which in the linear case is⁴:

$$\dot{x}(t) = A(\theta)x(t) + B(\theta)u(t) \quad (6)$$

$$T(t) = C(\theta)x(t) \quad (7)$$

where $x \in \mathbb{R}^n$ is the state vector composed of the temperature of the relevant thermal masses, n the order of the system, $u \in \mathbb{R}^p$ input vector, p the number of inputs, A the $n \times n$ system matrix, B the $n \times p$ input matrix, $\theta \in \mathbb{R}^m$ a vector of m model parameters, and $T(t)$ the TCL temperature in °C.

4.1.3. Model identification

As comprehensively described in [24, 27, 28], the adopted identification process consists in these steps:

- Experiments design: a series of dedicated off-line experiments are performed, where the TCL is controlled with a pseudo random binary signal (PRBS), a two levels on/off wave where duty cycles are of random durations. This has the objective of exciting a wide range of system dynamics. The measurement set is normally divided into a training and validation data set, the former used to fit model parameters and perform preliminary validation tests, and the latter for advanced validation.

⁴The feedforward matrix D is omitted.

- Model formulation: the mathematical formulation of the candidate model is developed. In this case, we adopt the thermal equivalent circuit formulation, as described in the previous paragraph.
- Parameters estimation: the parameters of the candidate model are estimated by maximizing the likelihood function of the one-step-ahead predictions through the software library CTSM [29, 30].
- Model validation: it mainly consists in evaluating if the candidate model can capture all the time dynamics contained in the training data set. This is performed by evaluating residual autocorrelation in time of the model one-step-ahead prediction errors. In the ideal case, this should not exhibit any predictable structure and behave as an independent and identically distributed (i.i.d.) random noise.
- Model extension: if the prediction errors are correlated in time, an alternative model should be formulated by, e.g., increasing the order of the candidate model or adopting an alternative mathematical description of the process. The extended candidate model should be estimated and validated by reiterating the procedures at the previous two points. The model extension can be cross-validated against the older candidate model by applying, e.g., the deviance test, to avoid model overfitting due to the increased number of parameters.

4.1.4. Electric space heating

We consider the third order linear thermal model developed in [27] for Power Flexhouse, an eight-room free standing office building where heat is provided by ten electric radiators, for a total nominal power of 10 kW. The temperature dynamics are described as a function of the radiators heating power, outside air temperature and solar radiation, and by using the approximation that the interior of the building is one room. We present the model formulation by referring to the state-space representation introduced in (6)-(7). The 3×1 input real vector at time t is:

$$u(t) = [s(t) \cdot P \quad T^o(t) \quad \phi(t)]^T \quad (8)$$

where $s(t)$ is the thermostat state as in Eq. (1), P is the total radiators heating power (kW), T^o the outside air temperature ($^{\circ}\text{C}$), ϕ the global horizontal irradiance (GHI, W m^{-2}). The system matrices are:

$$\begin{aligned} A &= \begin{bmatrix} \frac{-1}{C_i R_{ia}} + \frac{-1}{C_i R_{im}} + \frac{-1}{C_i R_{ih}} & \frac{1}{C_i R_{im}} & \frac{1}{C_i R_{ih}} \\ \frac{1}{C_m R_{im}} & \frac{-1}{C_m R_{im}} & 0 \\ \frac{1}{C_h R_{ih}} & 0 & \frac{-1}{C_h R_{ih}} \end{bmatrix} \\ B &= \begin{bmatrix} 0 & \frac{1}{C_i R_{ia}} & \frac{A_w}{C_i} \\ 0 & 0 & 0 \\ \frac{1}{C_h} & 0 & 0 \end{bmatrix} \\ C &= [1 \quad 0 \quad 0] \end{aligned} \quad (9)$$

where C_i, C_m, C_h are model parameters that describe the thermal capacities associated to the thermal masses of the building (building envelope, air content and radiators), R_{ia}, R_{im}, R_{ih} are the associated thermal resistance and A_w is the window area. Models are estimated from measurements of the total radiators electric power, indoor temperature, outdoor temperature and GHI, and their values are given in Table A.4.

4.1.5. Freezer

The model has been originally proposed in [24] and estimated from experimental temperature/power measurements of a 333 liters class A+ domestic freezer. Heat dynamics are described as a function of the power consumption, coefficient of performance (COP), and room temperature. The model input vector is:

$$u(t) = [s(t) \cdot P \quad T^r(t)]^T \quad (10)$$

where $s(t)$ is the thermostat state, P is the freezer nominal power (W), and $T^r(t)$ is the temperature of the room where the freezer is located. The system matrices are:

$$A = \begin{bmatrix} \frac{-1}{C_e R_e} & \frac{1}{C_e R_e} & 0 \\ \frac{1}{C_a R_e} & \frac{-1}{C_a R_a} + \frac{-1}{C_a R_e} & \frac{1}{C_a R_a} \\ 0 & \frac{1}{C_w R_a} & \frac{-1}{C_w R_w} + \frac{-1}{C_w R_a} \end{bmatrix} \quad (11)$$

$$B = \begin{bmatrix} 0 & -\eta \cdot \frac{\text{COP}(T^r(t), x_1(t))}{C_e} \\ 0 & 0 \\ \frac{1}{C_w R_w} & 0 \end{bmatrix} \quad (12)$$

$$C = [0 \quad 1 \quad 0], \quad (13)$$

where C_e, C_a, C_w are the thermal capacities of the freezer evaporator, air content, and freezer envelope, while R_e, R_a, R_w are the associated thermal masses. The term η is the fridge efficiency with respect to the ideal COP, which is modeled as the reversed Carnot cycle operating between the room and freezer evaporator temperatures (that is the first element of the state vector, denoted by $x_1(t)$). Formally, the COP in (12) is:

$$\text{COP}(T^r(t), x_1(t)) = \frac{x_1(t) + 273}{T^r(t) - x_1(t)} \quad (14)$$

The freezer model is nonlinear since the value of the state appears as a multiplicative factor of the input signal. The model parameters, estimated from measurements as described in [24], are summarized in Table A.5.

4.1.6. Fridge

This model is from [28] and was identified and estimated from experimental measurements from a 50 liters class A domestic fridge. The dynamic model is the same as for the freezer in the previous section, unless for the input matrix B , which in this case is:

$$B = \begin{bmatrix} 0 & -\text{COP} \\ 0 & 0 \\ \frac{1}{C_w R_w} & 0 \end{bmatrix} \quad (15)$$

where COP is a coefficient to estimate. In this case the model is linear: the reason for neglecting the nonlinear COP formulation is because fridges normally operates in a smaller temperature range than freezers, thus the nonlinearities in (14) play a minor role. Estimated model parameters are reported in Table A.6.

4.1.7. Electric water heater

The model refers to a 1.3 kW single element electric water heater. It is the first order model originally proposed in [10] and describes the global energy content in the water as function of the electricity consumption, water usage and thermal losses towards the exterior. A similar model was found in [31]. The model does not account for the thermal stratification of the water inside the tank, as attempted e.g. in [32]. The model inputs are:

$$u(t) = [s(t) \cdot P \quad T^r(t) \quad q(t)]^T \quad (16)$$

where $s(t)$ is the thermostat state, P is the heater nominal power, T^r is the temperature of the room where the heater is located, and q is the water consumption (L s^{-1}). The system matrices are:

$$A = -\frac{1}{R_e C_w} \quad (17)$$

$$B = \left[\frac{1}{C_w} \quad \frac{1}{R_e C_w} \quad \frac{C_p}{C_w} (T^w(t) - T(t)) \right] \quad (18)$$

where T_{inlet} is the temperature of the inlet water, and C_w and R_e are model parameters. The former denotes the lumped thermal capacity of the water heater: it is approximated by the thermal capacity associated to the water content, namely $4.2 \text{ kJ kg}^{-1} \text{ K}^{-1}$ per 30 kg of water mass, disregarding the tank structure and envelope (which should account for a smaller share, $\approx 0.8 \text{ kJ kg}^{-1} \text{ K}^{-1}$ assuming 3 kg of polyurethane foam as the insulation layer [33]). The thermal resistance R_e is estimated from experimental measurements by minimizing the sum of the squared prediction errors of the model. The value of R_e and C_w are summarized in Table A.7. We note that the model is nonlinear since the value of the temperature appears as an input in the matrix B.

4.2. Sampling of model inputs and parameters for Monte Carlo simulations

In order to determine the equivalent storage potential of the selected TCLs under different typical operating conditions, Monte Carlo simulations are performed where the uncontrollable model inputs and controller parameters are randomly sampled from relevant scenarios. The way the inputs and parameters are generated are explained in the following for each considered TCL.

4.2.1. Space heating inputs and parameters

The uncontrollable inputs of the electric space heating model are outdoor air temperature $T_{t_i}^o$ and global horizontal irradiance (GHI) ϕ_{t_i} . Both quantities are characterized by diurnal and seasonal variations, which need to be considered in the Monte Carlo simulations because they have a strong influence on the heat demand, and thus on the equivalent storage capacity inherent space heating operation. They are as:

- to capture diurnal variations, daily scenarios are daily time series measurements of GHI and outdoor air temperature from a local weather station (Risoe DTU, Roskilde, Denmark);
- seasonal variability is considered by taking into account two distinct cases thanks to using two groups of measurements recorded in different periods of the year, from 15 to 30 September 2013 (early autumn), and from 15 to 30 December 2013 (early winter).

Outdoor air temperature and GHI daily scenarios of the autumn case are exemplified in Fig. 2. Statistics and measurements periods of both winter and autumn cases are summarized in Table 2. As far as the parameters of the space heating thermostatic controller are concerned, they are normally according to consumer preferences. In this case, they are assumed randomly distributed according to the distributions specified in Table C.8.

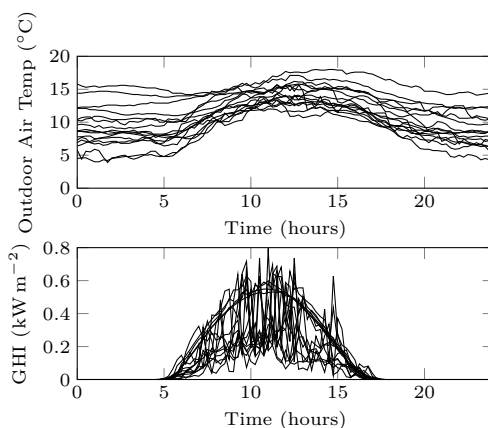


Figure 2: Daily scenarios of outdoor air temperature and GHI for the autumn case.

Table 2: Average values of outdoor air temperature and GHI over all possible daily scenarios.

Case	Period	Average Temperature (°C)	Average GHI (kW m ⁻²)
Autumn	15 to 30 Sep 2013	11.1	104.4
Winter	15 to 30 Dec 2013	2.0	30.1

4.2.2. Freezer and fridge inputs and parameters

The only non-controllable input of the freezer and fridge models is the room temperature T^r . It is assumed time invariant since refrigeration units normally operates in temperature-controlled environment and is sample from a normal distribution $\mathcal{N}(\mu, \sigma^2)$, with mean μ and standard deviation σ^2 as given in tables C.9 and C.10. The tables also show the value of the controller free parameters T^* and hysteresis h . They are chosen according to food storage recommendations [34].

4.2.3. Electric water heater inputs and parameters

The inputs of the water heater thermal model are the room temperature and water consumption profile. The former is chosen as done for the refrigeration units, while the latter is as in Table C.11, where q_{t_i} is the water consumption profile proposed in [35] and scaled to account to hot water demand of four people. It is exemplified in 3.

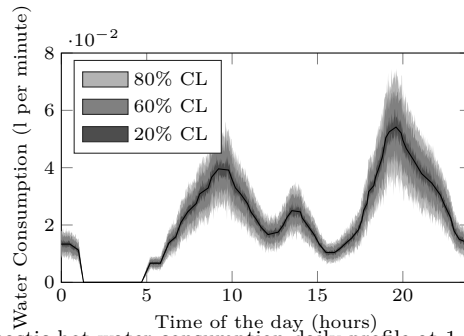


Figure 3: Stochastic hot water consumption daily profile at 1 minute resolution.

4.3. Evaluation of the equivalent storage capacity

For each considered TCL, Monte Carlo simulations are performed according to the procedure exemplified in Fig. 4 and described hereafter.

First, K input scenarios are generated off-line for each TCL (for space heating, the autumn and winter cases are analyzed in a separated fashion). Each scenario is composed of the relevant model input time series and parameters, randomly selected as described in the previous paragraph. Therefore, for each scenario $k = 1, \dots, K$ (K is the scenarios number and is given in Table 3), the TCL baseline temperature evolution as a function of the input scenario is computed for the time interval t_1, \dots, t_N (N , given in Table 3, is the number of simulation steps) by applying the models described in the previous section (discretized as shown in Appendix Appendix B) and while enforcing the thermostatic control law (1) at each time step. At this point, the operative definition of equivalent storage capacity given in Section 3 is applied:

- a random index i is sampled from an uniform distribution in the range $[1, N]$;
- the state of the TCL at time t_i is inverted (if *off* is forced to *on*, and viceversa) and a new perturbed temperature profile in the interval t_i, \dots, t_N is determined;

- the values t_i^\uparrow and t_i^\downarrow are extracted from the baseline and perturbed temperature evolutions by applying their (verbose) definition given in Section 2;
- the power and energy capacity available to increase or reduce consumption $P_i^\uparrow|k, E_i^\uparrow|k, P_i^\downarrow|k, E_i^\downarrow|k$ are determined by applying their respective definitions in (2)-(5), where the notation “ $|k$ ” stands for “given scenario k ”.

The procedure described in the previous 4 points is iterated for I (given in Table 3) times for as many random realizations of i .

Finally, the expected values of the TCL equivalent storage capacity for up and down-regulation for the input scenario k is obtained by averaging over i :

$$P^\downarrow|k = \frac{1}{I} \sum_{i=1}^I P_i^\downarrow|k \quad (19)$$

$$E^\downarrow|k = \frac{1}{I} \sum_{i=1}^I E_i^\downarrow|k \quad (20)$$

$$P^\uparrow|k = \frac{1}{I} \sum_{i=1}^I P_i^\uparrow|k \quad (21)$$

$$E^\uparrow|k = \frac{1}{I} \sum_{i=1}^I E_i^\uparrow|k \quad (22)$$

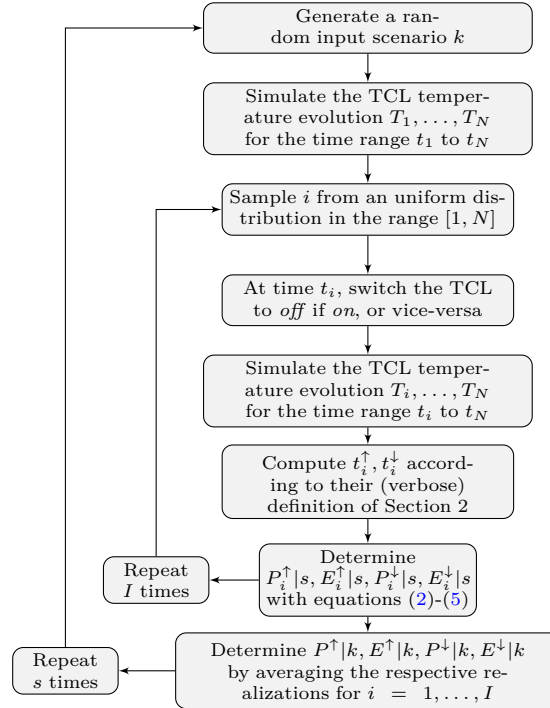


Figure 4: The procedure adopted to perform the Monte Carlo simulations and assess the equivalent storage capacity of the considered TCLs.

Table 3: Parameters for the Monte Carlo simulations.

	Description	Unit	Value
Δt	Simulation Sample time	s	300 (space heating)
			10 (freezer)
			10 (fridge)
			60 (water heater)
t_N	Simulation length	hours	48 (space heating)
			12 (freezer)
			12 (fridge)
			24 (water heater)
K	Input scenarios number	–	1000
I	Number of attempt	–	1000

5. Results and Discussion

5.1. Montecarlo Simulation Results

Figures 5, 7, 8 and 6 show the distributions of the equivalent storage capacities ($P^\downarrow, E^\downarrow$) and (P^\uparrow, E^\uparrow) for up and down-regulation, respectively, for each of the considered TCLs.

Recalling from the previous section and for the sake of clarity the couple ($P^\downarrow, E^\downarrow$) denotes the power and electricity consumption that can be harvested from a given TCL for up-regulation (decrease in consumption), and vice-versa for (P^\uparrow, E^\uparrow).

Equivalent storage capacities in figures 5-6 are shown in the form of histograms because they are calculated as a function of random input scenario: the outcomes are thus histograms showing the distributions of the equivalent storage capacity due to different operating conditions.

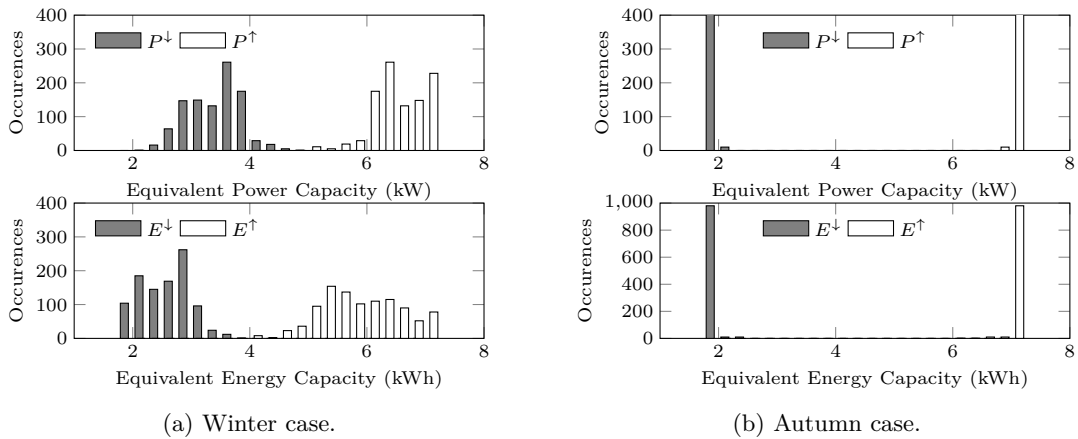


Figure 5: Space heating system: equivalent power and electricity storage capacity.

It can be noted from Fig. 5, which shows the results for the considered space heating system for the winter and autumn cases, that equivalent storage capacities available for up and down-regulation are different. This is because the ability of anticipating or deferring consumption depends on the TCL operating conditions. E.g., when considering space heating operation during a milder autumn day, the TCL duty cycle is characterized by a short warming up period and a very stretched cooling down phase due to reduced thermal losses towards the environment. In this case, the probability of the heating system being in the on state is low because the radiators are switched off for most of the time, thus resulting in lower values of P^\downarrow than P^\uparrow . This is also reflected on the value of the energy capacity, the activation of which depends on the

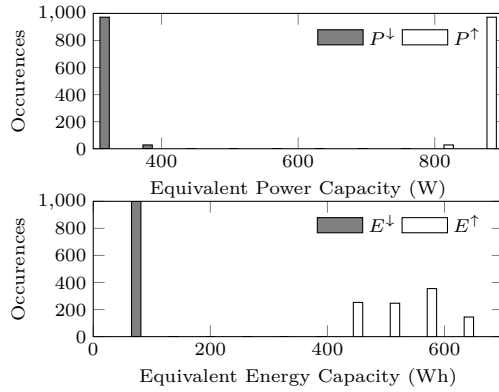


Figure 6: Electric water heater: equivalent power and electricity storage capacity for up and down regulation.

original state of the heating system. On the contrary, when considering a winter day, the power P^\downarrow and energy capacities E^\downarrow are larger than the previous case because the probability of the space heating system being on are higher.

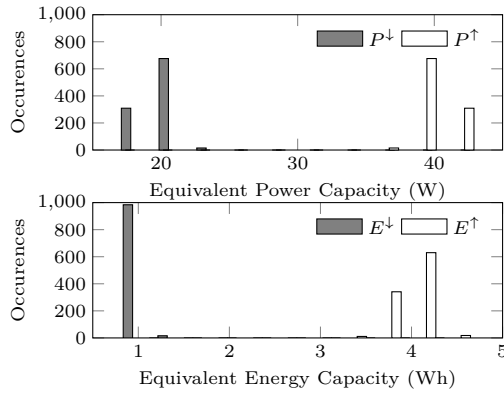


Figure 7: Freezer: equivalent power and electricity storage capacity for up and down regulation.

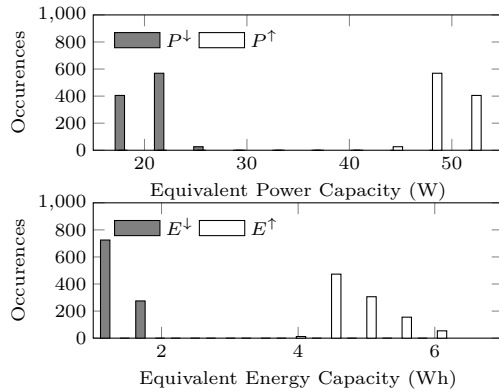


Figure 8: Fridge: equivalent power and electricity storage capacity for up and down regulation.

When considering the results for the freezer, fridge and water heater (figures 7-6), it can be observed that the respective equivalent storage capacities are considerably smaller than for the space heating. A

more thoughtful comparison between the equivalent storage capacities of the considered TCLs is the focus of the next paragraph, 5.2. Moreover, it can be noted the capacities of providing up and down-regulation are considerably asymmetric, with a larger capacity for the latter case.

5.2. Comparison with benchmark devices

In this section, the TCL equivalent storage capacities of the considered TCLs is compared against each other, and also against two benchmark storage devices, which correspond to two experimental grid-connected battery energy storage systems (BESSs). They are:

- 720 kVA/500 kWh lithium-ion BESS available at EPFL Distributed Electrical System Laboratory (see [36] for more details);
- 15 kVA/120 kWh Vanadium flow redox BESS available at DTU Elektro ([37]).

In this analysis, the equivalent storage capacity of each TCL (space heating autumn case, space heating winter case, freezer, fridge, water heater) for up and down-regulation is considered in terms of its *expected value*, which is calculated by considering the (empirical) probability density functions corresponding to the histograms in figures 5-6. In order to be consistent with the adopted “expected equivalent storage capacity” representation, BESSs are considered at 50% state-of-charge (SOC).

Fig. 9 compares the expected equivalent storage capacities of the considered devices. In order to further clarify the meaning of Fig. 9, each data point consists in couple of power and energy values, each calculated as the expected value of the respective histogram in figures 5-6. Each data point represents the storage capacity that one might expect from the respective device when it is activated to provide up or down-regulation. It is worth noting that equivalent storage capacity of TLCs is still strongly influenced by environment conditions (like weather patterns, as captured in the proposed Monte Carlo analysis): however, the main objective of this analysis is provide expected value to be used as a rule-of-thumb indicators to describe flexibility.

The representation in Fig. 9 and following figures is inspired from the Ragone plot, which, in its original form, it is used to compare power and energy densities of electrochemical storage technologies.

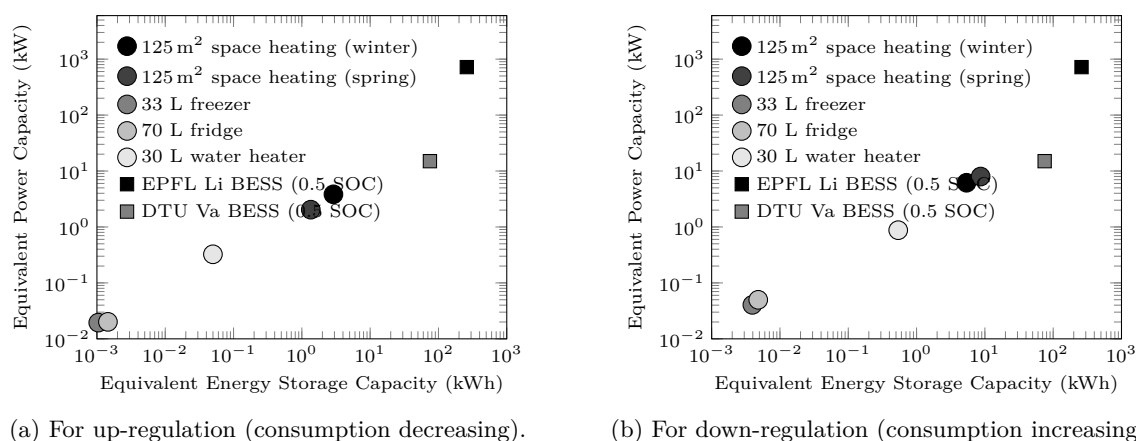


Figure 9: Power and energy capacities per device.

As visible from Fig. 9, the equivalent storage capacity of space heating is approximately two order of magnitude less than the largest considered battery system, meaning that the aggregation of several tens of units would lead to have a comparable level of storage capacity as utility-scale BESSs. However, it is to consider that the storage capacity of space heating has seasonal trends, while it is not for electrochemical storage.

As far as the freezer, fridge and water heaters are concerned, it can be seen from Fig. 9 that they can provide a little amount of flexibility. Although these TCLs are numerous in existing distribution networks, their use as a flexible resource is arguable when considering that harvesting their flexibility requires an

extended monitoring and control infrastructure and efficient aggregation algorithms. An elementary cost-benefit analysis to evaluate whether a demand response scheme is economically convenient compared to the deployment of utility-scale BESSs is proposed later in this paper, in paragraph 5.2.2.

5.2.1. Equivalent storage capacity per unit of occupied volume

Figure 10 shows the storage capacity per unit of volume of the considered devices. For each unit, it the ratio between the respective storage capacity and occupied volume. For the TCLs, we consider the sizes reported in Table 1, while, for the BESSs, we consider the real occupancy of the system (approximately 80 m^2 for the , and $6500\text{ L} \times 2$ for the reactants tanks plus 40 m^2 for the auxiliaries). As visible, the BESSs have larger specific capacities than flexible demand, therefore able to achieve larger storage capacities than for the same occupancy.

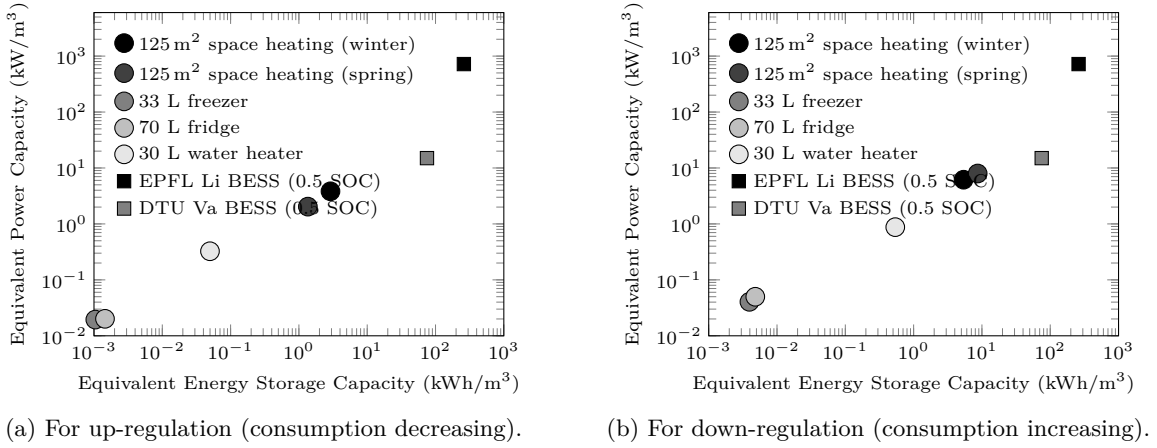


Figure 10: Power and energy capacities per unit of occupied volume.

5.2.2. Equivalent storage capacity per unit of capital investment cost

Figure 11 compares the equivalent storage capacities per unit of capital investment cost. The cost considered for BESS technologies is 800 and 500 EUR per kWh, for lithium-ion and vanadium redox, respectively. The capital investment cost for TCLs is given by implementing mechanisms for local monitoring and control of the thermostat, and it is assumed 100 EUR. The cost only includes local hardware, and not devices which might be necessary to implement aggregation at higher levels. As visible from Figure 11, the space heating system outperforms BESSs technologies, the water heater has comparable storage capacity per cost as BESSs, while the freezer and fridge appear to be not convenient compared to the others.

As a final consideration, it is worth to remark that storage capacity, although being a fundamental metric to quantify the flexibility inherent the operation of a given storage device or demand side resource, is not the only distinguishing factor to consider when planning storage. An important factor is the ability of BESSs to inject power into the grid, a relevant feature when considering power system restoration procedures. Also, flexible demand is subject to a baseline consumption to maintain a minimum consumers comfort level, whereas batteries system can postpone the charging demand to any time in the future. Finally, the requirements of the control framework are substantially different among the two considered cases. While in the case of utility-scale BESS, the control action is normally accomplished by sending a control signal to a single industrial-grade component, the case of flexible demand requires the simultaneous control of a large number of inherently stochastic units, and the tracking performance might be considerably different.

6. Conclusions

The definition of “equivalent storage capacity” for thermostatically controlled loads (TCLs) was given. It is defined as the amount of power and electricity consumption which can be deferred or anticipated in time

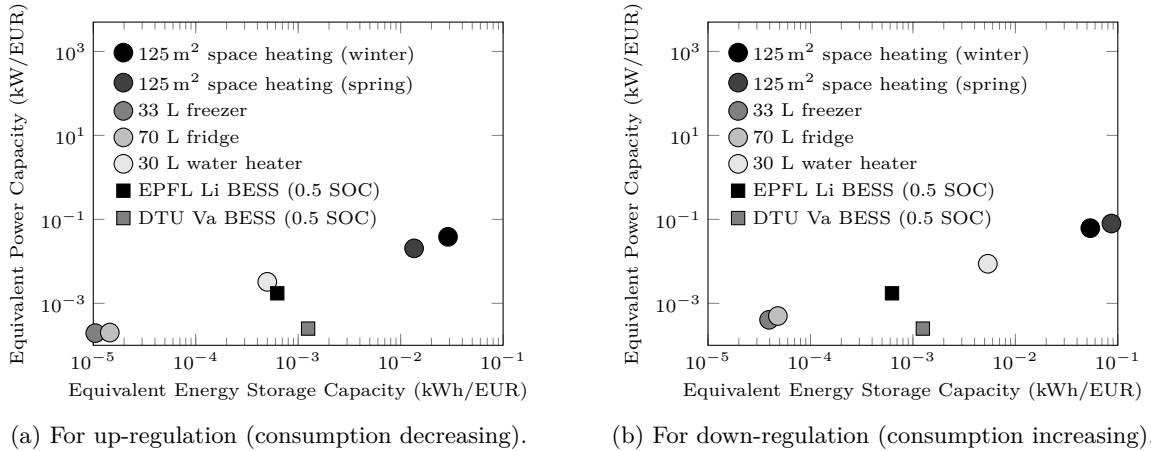


Figure 11: Power and energy capacities per unit of cost.

with respect to the baseline consumption (namely, when no demand side event occurs) without violating temperature thermostatic bounds.

An analytical formulation to determine the equivalent storage capacity was proposed and applied in Monte Carlo simulations to quantify the flexibility of selected thermostatic controlled loads: an electric radiators-based space heating system for a 125 m² free standing office building, 33 liters water heater, 333 liters freezer and 60 liters fridge. They were simulated by using dynamic grey-box thermal models identified from experimental measurements. Monte Carlo simulations were performed by sampling model inputs from relevant scenarios representative of typical TCLs operating conditions. This is of importance because flexibility normally depends on external conditions, such as – for space heating – solar irradiance and outdoor air temperature. Equivalent storage capacity analyses were performed considering up (i.e. capability of decreasing consumption) and down-regulation (vice-versa) in a separate fashion. Indeed, they can differ because unequal durations of the TCLs warming up/cooling down phases, which determine asymmetric probabilities of a TCL being on or off, thus impacting the support they can provide to one or the other service.

Based on the considered scenarios and models, simulation results show that the resource with highest average equivalent storage capacity is the electric space heating system, although it shows a significant seasonal variability. Seasonality is indeed an important element which should be certainly accounted for when planning the provision of power system ancillary services from flexible demand. The second TCL for largest equivalent storage capacity is the water heater, although remarkably asymmetric for up and down regulation. Finally, freezer and fridges ranked as last.

Based on these results, two performance comparisons with two grid-connected battery energy storage systems (BESSs), notably a 720 kVA/500 kWh Lithium ion and 15 kVA/120 kWh Vanadium flow redox battery, were performed. The first comparison concerned the evaluation of the equivalent storage capacity per unit of occupied volume, which shows that the considered BESSs are the units with largest energy and power densities.

The second comparison concerned the assessment of the economic cost per unit of storage capacity. The cost considered for the BESSs was the capital investment of the whole grid-connected battery system (800 EUR for lithium-ion and 500 EUR for Vanadium flow redox), while for TCLs the investment necessary to make the unit controllable (in fact, TCLs are already available in the consumption mix and only need an upgrade to enable the control). Assuming a TCL upgrade cost of 100 EUR, it was seen that the considered space heating system is the most cost-competitive storage solution, the water heater and electrochemical storage scored similar results, and freezer and fridge were the less competitive.

In general, it is to note that the proposed results are valid for the considered devices and simulation conditions. Nevertheless, the proposed method can be applied to estimate the flexibility of TCLs with dif-

ferent characteristics. Moreover, proposed results give reasonable approximations of the order of magnitude of the equivalent storage capacity of domestic TCLs and provide useful rule-of-thumb indicators to system planners to decide on the proper storage technology to use or on the optimal storage mix as a function of the ancillary service to provide.

Appendix A. TCLs Parameters

Tables A.4, A.5, A.6 and A.7 show the parameters adopted for the Monte Carlo simulations.

Table A.4: Space heating model parameters.

Parameter	Unit	Value
C_i	JK^{-1}	9.58×10^3
C_m	JK^{-1}	1.11×10^4
C_h	JK^{-1}	1.38×10^1
R_{ia}	KW^{-1}	4.82
R_{ih}	KW^{-1}	3.33×10^1
R_{im}	KW^{-1}	3.45
A_w	m^2	5.12

Table A.5: Freezer model parameters.

Parameter	Unit	Value
C_a	JK^{-1}	1.25×10^4
C_e	JK^{-1}	1.22×10^3
C_w	JK^{-1}	8.30×10^3
R_a	KW^{-1}	1.61×10^{-1}
R_e	KW^{-1}	1.47×10^{-1}
R_w	KW^{-1}	6.32×10^{-1}
η	-	5.67×10^{-1}

Table A.6: Fridge model parameters.

Parameter	Unit	Value
C_a	JK^{-1}	4.42×10^3
C_e	JK^{-1}	1.92×10^1
C_w	JK^{-1}	1.07×10^4
R_a	KW^{-1}	3.74
R_e	KW^{-1}	2.24
R_w	KW^{-1}	0.20
COP		5.67×10^{-1}

Table A.7: Electric water heater model parameters.

Parameter	Unit	Value
C_w	JK^{-1}	1.257×10^5
R_e	KW^{-1}	1.2

Appendix B. Models Discretization

Continuous time dynamic models in the form (6)-(7) are discretized by applying finite forward difference. In the case of linear models and referring to notation introduced (6)-(7), it is:

$$x_{i+1} = A_d x_i + B_d u_i \quad (\text{B.1})$$

$$T_i = C x_i, \quad (\text{B.2})$$

where $A_d = (A\Delta t + I_n)$, $B_d = B\Delta t$, Δt is the discretization interval and I_n denotes the $n \times n$ identity matrix. For the nonlinear models (freezer and water heater), the value of B_d is also updated according to the value of the state vector at time t_i . E.g., in the case of the water heater, B_d is:

$$B_d = \left[\frac{1}{C_w} \quad \frac{1}{R_e C_w} \quad \frac{C_p}{C_w} (T_{t_i}^w - T_{t_i}) \right] \Delta t. \quad (\text{B.3})$$

Also, the thermostatic control law in Eq. (1) is discretized as:

$$s(i) = \begin{cases} \text{on,} & T(i) \leq T^* + h \\ \text{off,} & T(i) > T^* - h \\ s(i-1), & \text{otherwise} \end{cases} \quad (\text{B.4})$$

Appendix C. Random scenarios for Monte Carlo simulations

Tables C.8, C.9, C.10 and C.11 show the parameters adopted for the Monte Carlo simulations.

Table C.8: Space heating parameters.

Symbol	Description	Unit	Value
T^*	Thermostatic set-point	$^{\circ}\text{C}$	$\mathcal{N}(21, 0.5^2)$
h	Thermostatic hysteresis	$^{\circ}\text{C}$	1.5

Table C.9: Freezer model inputs and parameters.

Symbol	Description	Unit	Value
T^r	Room temperature	$^{\circ}\text{C}$	$\mathcal{N}(21, 0.5^2)$
T^*	Thermostatic set-point	$^{\circ}\text{C}$	$\mathcal{N}(-20, 0.5^2)$
h	Thermostatic hysteresis	$^{\circ}\text{C}$	0.5

Table C.10: Fridge model inputs and parameters.

Symbol	Description	Unit	Value
T^r	Room temperature	$^{\circ}\text{C}$	$\mathcal{N}(21, 0.5^2)$
T^*	Thermostatic set-point	$^{\circ}\text{C}$	$\mathcal{N}(4, 0.5)$
h	Thermostatic hysteresis	$^{\circ}\text{C}$	0.5

Table C.11: Electric water heater model inputs and parameters.

Symbol	Description	Unit	Value
T^r	Room temperature	$^{\circ}\text{C}$	$\mathcal{N}(21, 0.5^2)$
Q_i	Hot water demand	L s^{-1}	from [35] (scaled for 2 people)
T^w	Inlet water temperature	$^{\circ}\text{C}$	$\mathcal{N}(21, 0.5^2)$
T^*	Thermostatic set-point	$^{\circ}\text{C}$	$\mathcal{N}(4, 0.5)$
h	Thermostatic hysteresis	$^{\circ}\text{C}$	0.5

References

- Callaway DS. Tapping the energy storage potential in electric loads to deliver load following and regulation, with application to wind energy. *Energy Conversion and Management* 2009;50(5).
- Borsche TS, de Santiago J, Andersson G. Stochastic control of cooling appliances under disturbances for primary frequency reserves. *Sustainable Energy, Grids and Networks* 2016;7:70–9. URL: <http://www.sciencedirect.com/science/article/pii/S2352467716300285>. doi:<http://dx.doi.org/10.1016/j.segan.2016.06.001>.
- Douglass P, Garcia-Valle R, Nyeng P, Ostergaard J, Togeby M. Smart demand for frequency regulation: Experimental results. *IEEE Transactions on Smart Grid*, 2013;4(3):1713–20. doi:[10.1109/TSG.2013.2259510](https://doi.org/10.1109/TSG.2013.2259510).
- Christakou K, Tomozei DC, Le Boudec JY, Paolone M. Gecn: Primary voltage control for active distribution networks via real-time demand-response. *IEEE Transactions on Smart Grid* 2013;PP(99).
- Lakshmanan V, Marinelli M, Hu J, Bindner HW. Provision of secondary frequency control via demand response activation on thermostatically controlled loads: Solutions and experiences from denmark. *Applied Energy* 2016;173:470–80.
- Rodríguez DIH, Hinker J, Myrzik JMA. On the problem formulation of model predictive control for demand response of a power-to-heat home microgrid. In: *2016 Power Systems Computation Conference (PSCC)*. 2016:1–8. doi:[10.1109/PSCC.2016.7541024](https://doi.org/10.1109/PSCC.2016.7541024).
- Vanhoudt D, Geysen D, Claessens B, Leemans F, Jespers L, Van Bael J. An actively controlled residential heat pump: Potential on peak shaving and maximization of self-consumption of renewable energy. *Renewable Energy* 2014;63:531–43.
- Graditi G, Ippolito M, Lamedica R, Piccolo A, Ruvio A, Santini E, Siano P, Zizzo G. Innovative control logics for a rational utilization of electric loads and air-conditioning systems in a residential building. *Energy and Buildings* 2015;102:1–17. URL: <http://www.sciencedirect.com/science/article/pii/S0378778815004004>. doi:<http://dx.doi.org/10.1016/j.enbuild.2015.05.027>.
- Castillo-Cagigal E, Caamaño-Martín A, Gutiérrez D, Masa-Bote F, Monasterio J, Porro E, Matallanas J, Jiménez-Leube . Self-consumption of pv electricity with active demand side management: The gedelos-pv system. In: *25th European Photovoltaic Solar Energy Conference*. 2010:.
- Sossan F, Kosek AM, Martinenas S, Marinelli M, Bindner HW. Scheduling of domestic water heater power demand for maximizing PV self-consumption using model predictive control. In: *IEEE International Conference on Innovative Smart Grid Technologies (ISGT)*. 2013:.
- Luthander R, Widén J, Nilsson D, Palm J. Photovoltaic self-consumption in buildings: A review. *Applied Energy* 2015;142:80–94.
- Nick M, Cherkaoui R, Paolone M. Optimal siting and sizing of distributed energy storage systems via alternating direction method of multipliers. *International Journal of Electrical Power & Energy Systems* 2015;72:33–9.
- Elnashar MM, Shatshat RE, Salama MM. Optimum siting and sizing of a large distributed generator in a mesh connected system. *Electric Power Systems Research* 2010;80(6):690–7. URL: <http://www.sciencedirect.com/science/article/pii/S0378779609002752>. doi:<http://dx.doi.org/10.1016/j.epsr.2009.10.034>.
- Graditi G, Ippolito M, Telaretti E, Zizzo G. Technical and economical assessment of distributed electrochemical storages for load shifting applications: An italian case study. *Renewable and Sustainable Energy Reviews* 2016;57:515–23. URL: <http://www.sciencedirect.com/science/article/pii/S1364032115015786>. doi:<http://dx.doi.org/10.1016/j.rser.2015.12.195>.
- Han X, Sossan F, Bindner H, You S, Hansen H, Cajar P. Load kick-back effects due to activation of demand. In: *Proceedings of 5th IEEE PES Innovative Smart Grid Technologies*. IEEE; 2014:.
- Mathieu J, Dyson M, Callaway D. Using residential electric loads for fast demand response: The potential resource and revenues, the costs, and policy recommendations. *Proceedings of the ACEEE Summer Study on Buildings, Pacific Grove, CA* 2012:.
- Kosek AM, Costanzo GT, Bindner HW, Gehrke O. An overview of demand side management control schemes for buildings in smart grids. In: *IEEE International Conference on Smart Energy Grid Engineering*. 2013:.
- Costanzo GT, Zhu G, Anjos MF, Savard G. A system architecture for autonomous demand side load management in smart buildings. *IEEE Transactions on Smart Grid* 2012;3:2157–65.

19. Du P, Lu N. Appliance commitment for household load scheduling. *IEEE transactions on Smart Grid* 2011;2(2):411–9.
20. Zong Y, Kullmann D, Thavlov A, Gehrke O, Bindner H. Application of model predictive control for active load management in a distributed power system with high wind penetration. *IEEE Transactions on Smart Grid* 2012;3.
21. Sossan F, Bindner H, Madsen H, Reyes L, Torregrossa D, Paolone M. A MPC replacement strategy for electric space heating including cogeneration of a fuel cell-electrolyzer system. *International Journal of Electrical Power & Energy Systems* 2013;.
22. Gehrke O, Kosek A, Svendsen M. Flexhouse-2-an open source building automation platform with a focus on flexible control: demo abstract. In: *Proceedings of the 1st ACM Conference on Embedded Systems for Energy-Efficient Buildings*. ACM; 2014:188–9.
23. Li X, Wen J. Review of building energy modeling for control and operation. *Renewable and Sustainable Energy Reviews* 2014;37:517–37.
24. Sossan F, Lakshmanan V, Costanzo GT, Marinelli M, Douglass PJ, Bindner H. Grey-box modelling of a household refrigeration unit using time series data in application to demand side management. *Sustainable Energy, Grids and Networks* 2016;5.
25. Li X, Wen J, Bai EW. Developing a whole building cooling energy forecasting model for on-line operation optimization using proactive system identification. *Applied Energy* 2016;164:69–88.
26. Ji Y, Xu P, Duan P, Lu X. Estimating hourly cooling load in commercial buildings using a thermal network model and electricity submetering data. *Applied Energy* 2016;169:309–23.
27. P. Bacher A, Thavlov HM. Benchmarking smart metering deployment in the eu-27 with a focus on electricity. Tech. Rep.; DTU-IMM; 2010.
28. Costanzo GT, Sossan F, Marinelli M, Bacher P, Madsen H. Grey-box modeling for system identification of household refrigerators: A step toward smart appliances. In: *IEEE International Youth Conference on Energy (IYCE)*. 2013;.
29. Kristensen NR, Madsen H. Continuous time stochastic modelling. 2003.
30. Juhl R, Kristensen NR, Bacher P, Kloppenborg J, Madsen H. CTSM-R User Guide 2013;.
31. Nehrir M, Jia R, Pierre D, Hammerstrom D. Power management of aggregate electric water heater loads by voltage control. In: *IEEE Power Engineering Society General Meeting*. 2007;.
32. Vanthournout K, D’hulst R, Geysen D, Jacobs G. A smart domestic hot water buffer. *IEEE Transactions on Smart Grid* 2012;3:2121–7.
33. Thermal insulation materials made of rigid polyurethane foam. Tech. Rep.; Federation of European Rigid Polyurethane Foam; 2006.
34. Are you storing food safely? Tech. Rep.; US Food and Drug Administration; 2015. URL: <http://goo.gl/7cScJf>.
35. Kalogirou S, Tripanagnostopoulos Y. Hybrid PV/T solar systems for domestic hot water and electricity production. *Energy Conversion and Management* 2006;.
36. Sossan F, Namor E, Cherkaoui R, Paolone M. Achieving the dispatchability of distribution feeders through prosumers data driven forecasting and model predictive control of electrochemical storage. *IEEE Transactions on Sustainable Energy* 2016;7(4):1762–77. doi:10.1109/TSTE.2016.2600103.
37. Bindner HW, Krog Ekman C, Gehrke O, Isleifsson FR. Characterization of vanadium flow battery. Tech. Rep.; Danmarks Tekniske Universitet, Risø Nationallaboratoriet for Bæredygtig Energi; 2010.